# Structural and magnetic properties of $Fe[Fe(CN)_6]\cdot 4H_2O$

Amit Kumar and S. M. Yusuf*
*Solid State Physics Division, Bhabha Atomic Research Centre, Mumbai 400085, India*

L. Keller
*Laboratory for Neutron Scattering, ETHZ & PSI, CH-5232 Villigen PSI, Switzerland*
(Received 20 August 2004; revised manuscript received 25 October 2004; published 23 February 2005)

We report the structural and magnetic properties of polycrystalline ferriferricyanide, $Fe[Fe(CN)_6]\cdot 4H_2O$. The room temperature neutron diffraction pattern of the sample was refined with space group $Fm3m$ by the Rietveld refinement technique. The Mössbauer spectrum of the sample at room temperature reveals the presence of low spin $Fe^{3+}$ ($Fe^{LS}$, $S=1/2$) and high spin $Fe^{3+}$ ($Fe^{HS}$, $S=5/2$) ions. The compound undergoes a paramagnetic to ferromagnetic phase transition at 17.4 K. Saturation magnetization at 2.3 K corresponds to parallel ordering of $Fe^{HS}$ and $Fe^{LS}$ spin only moments in $Fe[Fe(CN)_6]\cdot 4H_2O$. Neutron diffraction study at 1.5 K shows the ordered site moments of 5.0(2) and 0.8(2) $\mu_B$ for $Fe^{HS}$ and $Fe^{LS}$ ions, respectively, in $Fe^{HS}[Fe^{LS}(CN)_6]\cdot 4H_2O$. The coercive field of the compound is an order of magnitude higher than that of many other compounds in the Prussian Blue analog family. The observed branching between field-cooled and zero field-cooled magnetization below $T_C$ (=17.4 K) is ascribed due to magnetic domain kinetics under different cooling conditions and the presence of available vacant sites in the lattice for the water molecules.

DOI: 10.1103/PhysRevB.71.054414 PACS number(s): 75.50.Xx, 61.12.Ld, 75.25.+z

## I. INTRODUCTION

Recently, there has been intense research in the field of molecular magnets[1–3] based on hexacyanometalates.[3–9] The general interest in this field is to control the magnetic properties like transition temperature, saturation magnetization, and coercive field and to combine magnetic properties with mechanical, electrical, and optical properties for practical application of these materials. Hexacyanometallates can be represented by the general formula $M'_x[M''(CN)_6]_y\cdot zH_2O$, where $M'$ and $M''$ are $3d$ transition metal ions. Hexacyanometallates possess fcc structure in which $M'$ and $M''$ are surrounded octahedrally by N and C atoms, respectively. When $x/y=1$, the first coordination of $M'$ and $M''$ is $\{M'(NC)_6\}$ and $\{M''(CN)_6\}$, respectively. Water molecules, in this case, occupy the interstitial positions. But when $x/y>1$, some of the $\{M''(CN)_6\}$ vacancies are filled by water molecules and the first coordination of $M'$ and $M''$ are $\{M'(NC)_{6-n}(H_2O)_n\}$ $(n=1-6)$ and $\{M''(CN)_6\}$, respectively. In the later case $(x/y>1)$, there are two types of water molecules: (i) water molecules coordinated to $M'$ octahedra at empty nitrogen sites, and (ii) uncoordinated water molecules at interstitial positions.[10] The $M''$ ion surrounded by carbon octahedra experiences a strong ligand field and is expected to possess low spin configuration. On the other hand, the $M'$ ion surrounded by nitrogen octahedra sees a moderate or weak ligand field and is, therefore, expected to possess high spin configuration.[10]

Prussian Blue,[11–13] $Fe_4[Fe(CN)_6]_3\cdot 14H_2O$, is the parent compound of the family of hexacyanometallates. Ferromagnetic ordering temperature for Prussian Blue is very low ($T_C=5.6$ K) because low spin $Fe^{2+}$ ion ($t_{2g}^6\, e_g^0$, $S=0$) is diamagnetic and distance between two nearest high spin $Fe^{3+}$ ions ($t_{2g}^3\, e_g^2$, $S=5/2$) is large (10.16 Å)[11,12] along the $Fe^{2+}$-C≡N-$Fe^{3+}$ chain. Its transition temperature is too low for practical applications. Transition temperature of Prussian Blue can be enhanced by incorporating a paramagnetic ion at the diamagnetic $Fe^{2+}$ site. Using this strategy we have prepared a Prussian Blue analog compound, ferriferricyanide $Fe[Fe(CN)_6]\cdot xH_2O$ with both Fe ions in +3 ionic state. Bozorth *et al.*[14] reported the results of dc magnetization measurements ($T_C=22$ K, saturation magnetization$=3.8$ $\mu_B$/f.u.) on the "ferriferricyanide." However, the samples studied by them were not in single phase. Moreover, the exact chemical formula of the prepared sample for their study was not known. As ferriferricyanide forms one of the basic compounds in molecular based hexacyanometallates category, it is, therefore, quite important to understand the true nature of magnetic ordering in this fundamental molecular based magnetic material. With this aim, we have carried out structural and magnetic studies of single-phase ferriferricyanide, $Fe[Fe(CN)_6]\cdot xH_2O$ and the results of our study are reported here.

## II. EXPERIMENT

Ferriferricyanide was prepared by the precipitation method. In this method 100 ml 0.1 M $K_3Fe(CN)_6$ aqueous solution was slowly added to 200 ml 0.1 M $FeCl_3$ aqueous solution and the resulting solution was heated up to 53 °C. The hot solution was allowed to cool at room temperature and diluted to double of its initial volume after cooling. Dark green precipitate, so obtained, was filtered, washed many times with demineralized water and acetone and finally allowed to dry in air. The sample was ground to very fine powder. Neutron diffraction pattern, at room temperature, of the prepared polycrystalline sample was recorded using a one-dimensional (1D) position sensitive detector based powder diffractometer ($\lambda=1.249$ Å) at Dhruva Reactor, Trombay. Low temperature (1.5 and 50 K) neutron diffraction data

 

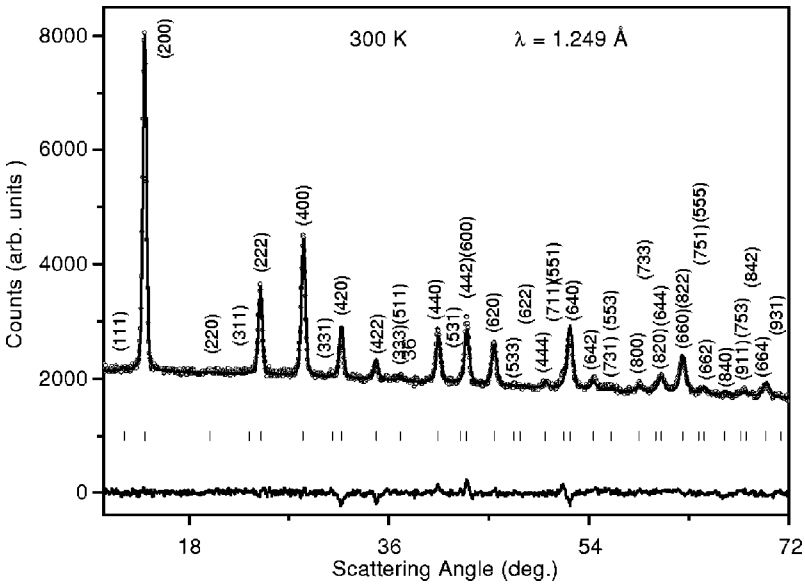


FIG. 1. Room temperature neutron diffraction pattern of ferriferricyanide. Open circles show observed data and solid line represents the Rietveld refined pattern. The difference pattern is shown in solid line below the Bragg peak markers (short vertical lines). The (*hkl*) values of all the Bragg peaks are also indicated.

were collected at DMC cold neutron powder diffractometer ($\lambda = 2.568$ Å), SINQ, Paul Scherrer Institute, Switzerland. Room temperature Mössbauer spectrum was recorded using a constant acceleration derive unit coupled with multichannel analyzer operated in time mode. dc magnetization measurements were carried out using a 12 T commercial (Oxford Instruments) vibrating sample magnetometer as a function of magnetic field and temperature. The sample taken for the magnetization measurements was in the form of a pellet weighing 20 mg. Temperature dependent magnetization measurements were carried out in field-cooled (FC) and zero field-cooled (ZFC) conditions down to 2 K. In ZFC conditions, first, the sample was cooled in the absence of magnetic field from room temperature down to the lowest temperature, then magnetization was measured as a function of temperature under the application of magnetic field in the heating cycle. In FC conditions, the sample was cooled down to 2 K in the presence of same magnetic field as used as a measuring field in the ZFC case and magnetization was measured (keeping the field on) as a function of temperature in the heating cycle. Hysteresis curves were recorded at several temperatures over +50 to −50 kOe field.

### III. RESULTS AND DISCUSSION

Figure 1 shows the observed room temperature neutron diffraction pattern of the prepared polycrystalline sample of ferriferricyanide. The diffraction pattern was analyzed by the Rietveld refinement technique using FULLPROF program.[15] Single phase formation of the ferriferricyanide was confirmed. The pattern could be indexed with the *Fm*3*m* space group. Starting values for the positions of carbon, nitrogen, and water molecules were taken from the literature.[11] Owing to the high background and limitations of powder diffraction, we treated water molecules as pseudoatoms $\{H_2O\}$ with an average scattering length $b(H_2O) = b(O) + 2b(H) = -1.68$ fm. In our refinement the best fitting was achieved by taking four water molecules per formula unit. Results of the analysis are listed in Table I. Figure 2 shows the unit cell of ferriferricyanide. The structure of the ferriferricyanide contains a three-dimensional network of $Fe_1$-N≡C-$Fe_2$ chains along the edges of the unit cell cube. The four water molecules present in the formula unit are uncoordinated and may be considered as zeolitic water. The distances between various atoms obtained from the analysis are $Fe_1$-N = 2.002(6) Å, $Fe_2$-C = 1.920(6) Å, C-N = 1.16(2) Å, $Fe_1$-$Fe_2$ = $a/2$ = 5.1090(5) Å, and $Fe_1$-$Fe_1$ = $Fe_2$-$Fe_2$ = $a$ = 10.218(1) Å, where $Fe_1$ and $Fe_2$ are Fe atoms at (0, 0, 0) and (1/2, 1/2, 1/2), respectively (see Table I). The derived values of interatomic distances are close to the values re-

TABLE I. Structural parameters for ferriferricyanide at room temperature.

| Space group = *Fm*3*m*, *a* = 10.218(1) Å, *Z* = 4 | | | | | |
|---|---|---|---|---|---|
| Atoms | *x* | *y* | *z* | Occupancy | *B* (Å$^2$) |
| $Fe_1$ | 0 | 0 | 0 | 1 | 0.5(1) |
| $Fe_2$ | 1/2 | 1/2 | 1/2 | 1 | 0.5(1) |
| C | 0.312(1) | 0 | 0 | 6 | 2.2(2) |
| N | 0.196(1) | 0 | 0 | 6 | 2.2(2) |
| $\{H_2O\}$ | 0.331(9) | 0.331(9) | 0.331(9) | 4 | 20(1) |
| $R_p = 1.54\%$, $R_{wp} = 2.44\%$, $R_{exp} = 2.30\%$ | | | | | |

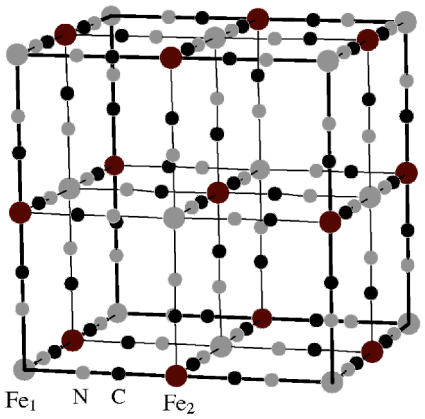


FIG. 2. Unit cell of $Fe[Fe(CN)_6]\cdot 4H_2O$. $Fe_1$ and $Fe_2$ represent $Fe^{3+}$ ions at (0, 0, 0) and (1/2,1/2,1/2) with $Fm3m$ space group symmetry, respectively. Water molecules are omitted for clarity.

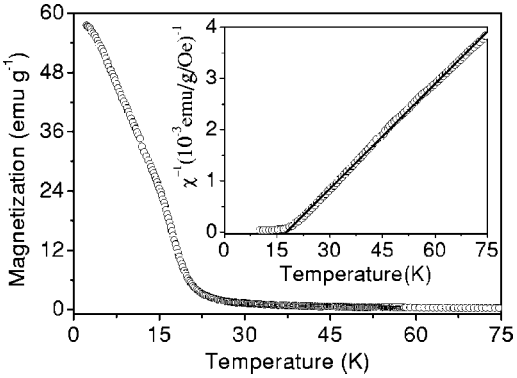


FIG. 4. FC magnetization vs temperature curve at 1 kOe field. Inset shows the inverse susceptibility vs temperature curve. Solid line is the Curie-Weiss fit in the temperature range 30–75 K.

ported for the parent Prussian Blue compound, $Fe_4[Fe(CN)_6]_3\cdot 14H_2O$.[11]

The room temperature Mössbauer spectrum of the prepared ferriferricyanide is shown in Fig. 3. The observed spectra can be fitted with two components having chemical shifts (CS) of −0.168 and 0.237 mm/s and quadrupole splitting (QS) of 0.27 and 0.45 mm/s, respectively. Linewidths for these two components are 0.364 and 0.444 mm/s, respectively. The component with CS=−0.168 mm/s and QS=0.27 mm/s may be identified as low spin $Fe^{3+}$ ($S=1/2$). Similar values of CS were found in the case of $K_{0.2}Co_{1.4}[Fe(CN)_6]\cdot 7H_2O$ (low spin $Fe^{3+}$, CS=−0.15 mm/s),[16] $Cu_{1.5}[Fe(CN)_6]\cdot 6H_2O$ (low spin $Fe^{3+}$, CS=−0.15 mm/s)[17] and $K_{0.8}Ni_{1.1}[Fe(CN)_6]\cdot 4.5H_2O$ (low spin $Fe^{3+}$, CS=−0.15 mm/s).[18,19] The second doublet with CS=0.237 mm/s and QS=0.45 mm/s may be identified as high spin $Fe^{3+}$ ($S=5/2$). The obtained value of CS is consistent with the value obtained from $K_{0.2}Co_{1.4}[Fe(CN)_6]\cdot 7H_2O$ (high spin $Fe^{3+}$, CS=0.19 mm/s).[16] Here we would like to mention that there is a "singlet" appearance for the component with QS=0.27 mm/s. Since linewidths for both the components are comparable with the linewidth (=0.30 mm/s) for iron foil used for calibration spectrum at room temperature, the apparent singlet behavior is not due to a large linewidth. This is, therefore, due to weak electric field gradient for this particular component that causes smaller QS.

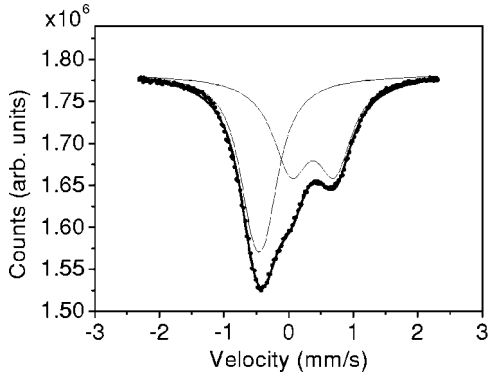


FIG. 3. Mössbauer spectrum of ferriferricyanide at room temperature. Open circles show the observed data and the thick solid line is the least square fitted curve. Two thin solid lines represent the components of the least square fitted curve.

It is seen from Fig. 2 that $Fe_1$ and $Fe_2$ are surrounded octahedrally by N and C atoms, respectively. Octahedral crystalline field splits the 3$d$ orbitals of $Fe^{3+}(d^5)$ ion into low energy $t_{2g}$ ($d_{xy}$, $d_{yz}$, $d_{zx}$) and high energy $e_g$ ($d_{z2}$, $d_{(x2-y2)}$) orbitals. It is evident from the interatomic distances that nitrogen octahedra are slightly bigger (3%) than the carbon octahedra. It is expected that $Fe_2$ should be affected by a stronger ligand field than $Fe_1$. The ligand field influences the spin configuration of the $Fe^{3+}$ ions directly. It induces high spin configuration ($t_{2g}^3\, e_g^2$, $S=5/2$) in $Fe_1$ ($Fe^{HS}$) and low spin configuration ($t_{2g}^5\, e_g^0$, $S=1/2$) in $Fe_2$ ($Fe^{LS}$).[10]

The observed negative chemical shift for the low spin $Fe^{3+}$ ion may be explained by the following way. N atom is more electronegative than C atom. When $Fe^{3+}$ ion is bonded to C atom, as in $[Fe(CN)_6]^{3-}$, 3$d$ electron density tends to flow from $Fe^{3+}$ ion to carbon atom along the Fe-C≡N chain due to the higher electronegativity of nitrogen atom. Due to reduced charge density of 3$d$ electrons at the $Fe^{3+}$ site, the shielding of 4$s$ electrons of $Fe^{3+}$ ion by its 3$d$ electrons becomes less effective. Hence, it increases the $s$-electron charge density at nucleus of $Fe^{3+}$ as compared to standard metallic iron. The increasing $s$-electron density at $^{57}Fe$ nucleus is responsible for the observed negative CS. On the other hand, no negative CS was observed for the high spin $Fe^{3+}$ ion. This is due to the fact that the high spin $Fe^{3+}$ ion experiences a weaker electronegativity effect as the size of the octahedron for this high spin $Fe^{3+}$ ion is 3% larger.

Figure 4 depicts the field-cooled magnetization ($M$) versus temperature ($T$) curve at 1 kOe magnetic field ($H$) in the temperature range 2–75 K. A sharp rise in $M$ is observed around 20 K. A transition temperature of 17.4 K was estimated from the minima of $dM/dT$ vs $T$ curve which corresponds to the steepest rise of $M$ with decreasing $T$. High temperature dc susceptibility ($\chi=M/H$) is found to obey the Curie-Weiss law

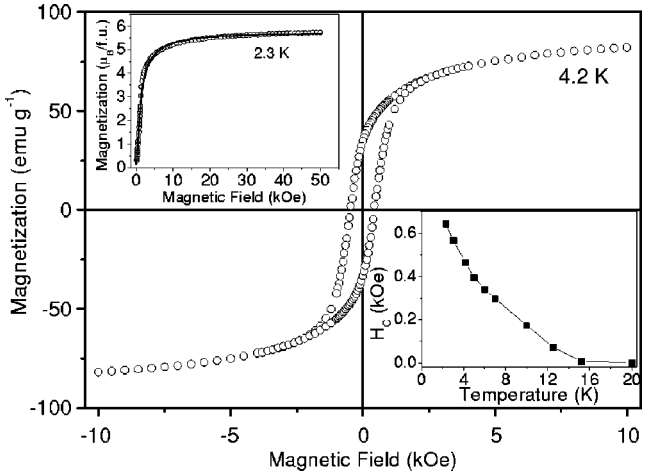


FIG. 5. Hysteresis curve at 4.2 K. Top inset shows the virgin $M$ vs $H$ curve at 2.3 K and solid line is the fit of the curve under mean field approximation (see text). Bottom inset shows the $H_C$ vs $T$ (solid line is drawn to guide the eyes).

$$\chi = \frac{C}{T - \Theta}, \tag{1}$$

where $C$ is Curie constant and $\Theta$ is paramagnetic Curie temperature. A linear fit of $\chi^{-1}$ vs $T$ curve in the temperature range 30–75 K is shown in the inset of Fig. 4. Fitting yielded $C = 4.974 \pm 0.002$ emu K/mole/Oe and $\Theta = 17.65 \pm 0.03$ K. The positive value of $\Theta$ indicates positive exchange correlations between the $Fe^{3+}$ ions. The effective magnetic moment in the paramagnetic state, $\mu_{\text{eff}}$, obtained from Curie constant is $(\mu_{\text{eff}})^2 = (3Ck_B/N_A\mu^2{}_B \sim 8C) = 39.79\ \mu^2{}_B$ (i.e., $\mu_{\text{eff}} = 6.31\mu_B$) per formula unit. This value is lower than the reported value ($\mu_{\text{eff}} = 6.8\ \mu_B$) for the "ferriferricyanide" system by Bozorth *et al.*[14] The theoretically expected spin only value of $(\mu_{\text{eff}})^2$ per formula unit can be calculated by using the formula $(\mu_{\text{eff}})^2 = \Sigma[g^2\{n.S.(S+1)\}]\ \mu^2{}_B$, where $g$ is gyromagnetic ratio ($\approx 2$), $n$ is the number of atoms/ions with spin $S$, and summation is over all magnetic atoms in the formula unit. There are only two magnetic atoms in one formula unit of $Fe[Fe(CN)_6]\cdot 4H_2O$, namely $Fe_1$ ($S = 5/2$) and $Fe_2$ ($S = 1/2$). The expected theoretical $(\mu_{\text{eff}})^2$, therefore, from spin only value is: $2^2\ (1 \times 5/2 \times 7/2)\ \mu^2{}_B + 2^2\ (1 \times 1/2 \times 3/2)\ \mu^2{}_B = 38\ \mu^2{}_B$. The observed value of $(\mu_{\text{eff}})^2$ is very close to the theoretically expected from spin only values (low spin and high spin) that indicates the total quenching of orbital moments. The quenching of the orbital moment in the iron-group metal ions is expected due to large spatial extent of 3$d$ shell and due to lack of outer electronic shells to screen the 3$d$ shell. The quenching of orbital moment is observed in many compounds of hexacyanometallate family.[3,7,17,20,21]

Hysteresis curve over ±10 kOe at 4.2 K is shown in Fig. 5. Large hysteresis (with a coercive field of 465 Oe and remanent magnetization of 34.58 emu/g), which is a characteristic of bulk ferro or ferrimagnetic type of ordering, is evident. Bottom inset in Fig. 5 shows the temperature dependence of coercive field, $H_C$. An increase in $H_C$ with lowering the temperature is evident. The observed value of $H_C$ is an order of magnitude higher than that for many other hexacyanometallates. For example, the observed value of $H_C$ for $V[Cr(CN)_6]_{0.86}\cdot 2.8H_2O$ is 25 Oe (at 10 K),[3] for $Cr_3[Cr(CN)_6]_2\cdot 10H_2O$ is 20 Oe (at 5 K)[5] and for $CsNi[Cr(CN)_6]\cdot 2H_2O$ is 71 Oe (at 3 K).[7] Higher $H_C$ values were also found for $Cu_{1.5}[Fe(CN)_6]\cdot 6H_2O$ ($H_C = 240$ Oe, at 4 K),[17] $CsCo[Cr(CN)_6]\cdot 0.5H_2O$ ($H_C = 800$ Oe, at 5 K),[21] and $KCo[Fe(CN)_6]$ ($H_C = 930$ Oe, at 4.2 K).[22] Top inset in Fig. 5 depicts virgin $M$ vs $H$ curve at 2.3 K. The magnetization is nearly saturated at 50 kOe field. The solid line represents the fitting of $M$ vs $H$ curve at 2.3 K under mean field approximation using the relationship

$$M = M_S B_S(x), \tag{2}$$

where $B_S(x)$ is Brillouin function

$$B_S(x) = \frac{2S+1}{2S}\,Coth\left(\frac{2S+1}{2S}x\right) - \frac{1}{2S}\,Coth\left(\frac{x}{2S}\right)$$

and

$$x = g\mu_B S(H + \lambda M)/k_B T.$$

Here, $M_S$ is saturation magnetization, $S$ is spin angular momentum quantum number, $k_B$ is Boltzmann constant, and $\lambda$ is mean field constant. The fit shown in the figure is obtained by taking $g = 2$ and $S = 3$ and varying $\lambda$ and $M_S$. Best fitting yielded $\lambda = 5.2(1)$ and $M_S = 5.84(2)\ \mu_B$/f.u. The observed value of saturation magnetization at 2.3 K is quite high compared to the value $M_S = 3.8\ \mu_B$/f.u., reported by Bozorth *et al.* in the literature.[14] The expected spin only value of ordered magnetic moment from collinear ferromagnetic ordering of $Fe_1$ ($S = 5/2$) and $Fe_2$ ($S = 1/2$) in $Fe[Fe(CN)_6]4H_2O$ is $\mu_S = (1 \times 2 \times 5/2 + 1 \times 2 \times 1/2)\ \mu_B = 6\ \mu_B$/f.u. This value is very close to our experimentally observed value of $M_S$ (5.8 $\mu_B$/f.u.) indicating a ferromagnetic ordering of spin only moments of ferriferricyanide, $Fe[Fe(CN)_6]\cdot 4H_2O$.

Figure 6 depicts the neutron diffraction patterns at 50 and 1.5 K. At 1.5 K, some intensity enhancement in low angle fundamental (nuclear) Bragg peaks is observed which indicates the presence of long range ferromagnetic ordering. Rietveld refinement with $Fm3m$ space group yielded 5.0(2) $\mu_B$ moment for $Fe^{3+}$ at (0, 0, 0) and 0.8(2) $\mu_B$ moment for $Fe^{3+}$ at (1/2,1/2,1/2) at 1.5 K. Moments lie along the crystallographic axes. The theoretically expected values of ordered moments for high spin and low spin $Fe^{3+}$ ions are 5 and 1 $\mu_B$, respectively. Ordered site moments obtained from the neutron diffraction study confirm the ferromagnetic ordering of $Fe_1$ ($S = 5/2$) at (0, 0, 0) and $Fe_2$ ($S = 1/2$) at (1/2,1/2,1/2) site moments.

Figure 7 shows the FC and ZFC magnetization as a function of temperature. At a field of 200 Oe, there is a clear branching between FC and ZFC magnetization curves. This branching diminishes as we increase the field and vanishes at ~5 kOe field. The temperature at which branching occurs (branching temperature) is also found to decrease with increasing magnetic field. This type of branching between FC and ZFC magnetization curves is very common in spin glass,[23–27] cluster spin glass,[28,29] and superparamagnets.[30–32]

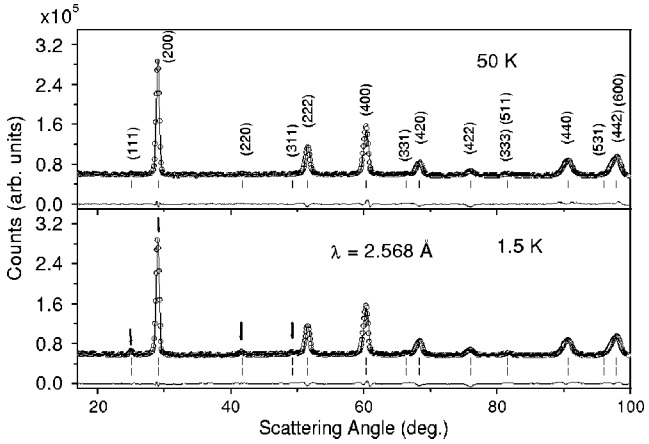


FIG. 6. Neutron diffraction patterns at 50 and 1.5 K. Observed data are shown by the open circles. Solid lines represent the calculated patterns. The difference patterns are shown at the bottom for each temperature. Short vertical lines represent the positions of Bragg peaks. The (*hkl*) values of all the Bragg peaks are also indicated. The Bragg peaks, marked by the vertically down arrows, receive considerable magnetic contribution at 1.5 K.

However, for the systems where long-range order is involved, the branching can occur from domains, domain walls, inhomogeneities and also from disorder.[33–36] From dc magnetization and low temperature neutron diffraction studies, it is clearly evident that ferriferricyanide belongs to a collinear ferromagnetic material with long-range correlation and higher coercivity. Here, the observed irreversibility between FC and ZFC magnetization curves might arise from domain mobility or domain growth under different cooling conditions. When the sample is cooled in the absence of magnetic field, the domains are more random giving low net magnetization. In the field-cooled case, however, magnetic domains are preferentially oriented in the direction of the applied magnetic field, thus giving higher value of magnetization. The other reasons for the observed branching could be due to the presence of inhomogeneity and inherent structural disorder. As far as the question of large inhomogeneity is concerned, this possibility is quite rare in our case as the sample was prepared by the precipitation method in which two homogeneous aqueous solutions of the reactants were mixed together to get the desired precipitate. However, the available interstitial vacant sites for the water molecules could be one of the contributing factors towards the observed branching in FC-ZFC magnetization curves. It is evident from our structural study that the high spin and low spin $Fe^{3+}$ ions occupy 4*a* (0, 0, 0) and 4*b* (1/2,1/2,1/2) crystallographic sites and the occupancies of these sites are 100%. Similarly, carbon and nitrogen atoms also occupy the 24*e* crystallographic site with 100% occupancies. However, water molecules occupy the 32*f* crystallographic site with only 50% occupancy. Therefore, a random distribution of water molecules (present in this compound) also contributes to the observed branching between the FC and ZFC magnetization curves.

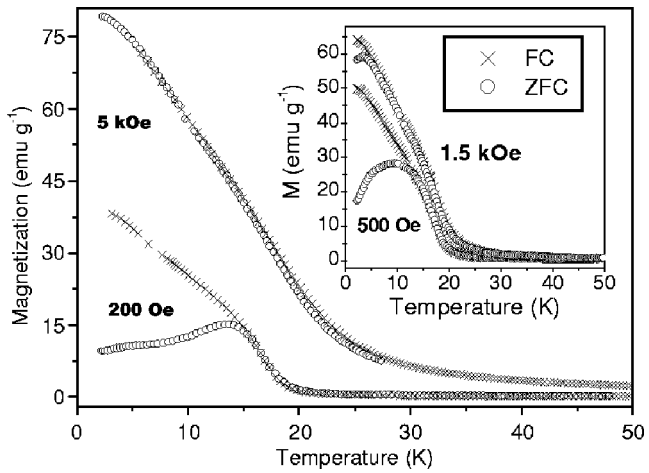


FIG. 7. Temperature dependence of $M_{ZFC}$ and $M_{FC}$ under the external magnetic field of $H=0.2$, 0.5, 1.5, and 5 kOe.

The observed ferromagnetism in $Fe[Fe(CN)_6]\cdot 4H_2O$ can be understood qualitatively on the basis of molecular-field theory. The octahedral crystalline field of $CN^-$ ligand splits the 3*d* orbitals of $Fe^{3+}$ into low energy $t_{2g}$ ($d_{xy}, d_{yz}, d_{zx}$) and high energy $e_g$ ($d_{z2}, d_{(x2\text{-}y2)}$) orbitals. Competition between splitting energy (difference in energy of $t_{2g}$ and $e_g$ orbitals) and pairing energy (energy required for pairing of electrons in an orbital) determines the spin state of $Fe^{3+}$ ion. In low spin configuration, splitting energy is higher than pairing energy so that pairing starts in $t_{2g}$ orbitals after the arrival of the fourth electron. The electronic configuration of low spin $Fe^{3+}(d^5)$, therefore, is $t_{2g}{}^5\, e_g{}^0$, i.e., there is only one unpaired electron and the resulting spin is $S=1/2$. In high spin configuration, on the other hand, splitting energy is lower than the pairing energy so that electrons can occupy high energy $e_g$ orbitals and the pairing of electrons in $t_{2g}$ and $e_g$ orbitals starts after the arrival of the sixth electron. The electronic configuration of high spin $Fe^{3+}(d^5)$, therefore, is $t_{2g}{}^3\, e_g{}^2$, i.e., there are five unpaired electrons in five orbitals and the resulting spin is $S=5/2$. The possibility of direct exchange between the two nearest magnetic ions is excluded because of large distances between them ($Fe_1$-$Fe_2$=5.109 Å). Large separation eliminates the possibility of direct overlap of magnetic orbitals of $Fe_1$ and $Fe_2$ ions, which is essential for direct exchange to take place. But the two magnetic ions can interact via cyanide ligand and this type of interaction is called superexchange interaction. The observed magnetism of ferriferricyanide, therefore, originates from superexchange interactions between the nearest high spin $Fe^{3+}(Fe_1)$ and low spin $Fe^{3+}(Fe_2)$ ions. These superexchange interactions are mediated by cyanide ligands. Contributions due to the second nearest neighbors can be neglected because of long distances between them ($Fe_1$-$Fe_1$=$Fe_2$-$Fe_2$=10.218 Å). The superexchange interactions may be positive or negative depending upon the symmetries of the magnetic orbitals involved. Ferromagnetic coupling occurs when the magnetic orbitals have different symmetries, e.g., between $d_{xy}$ ($t_{2g}$) orbital of $Fe_2$ and $d_{z2}$ ($e_g$) orbital of $Fe_1$ also between $d_{xy}$ ($t_{2g}$) orbital of $Fe_2$ and $d_{yz}$ ($t_{2g}$) orbital of $Fe_1$; whereas antiferromagnetic coupling results between the magnetic orbitals of same symmetry, e.g., $d_{xy}$ ($t_{2g}$) orbital $Fe_2$ and $d_{xy}$ ($t_{2g}$) orbital of $Fe_1$.[21] The systematic illustration of ferro and an-

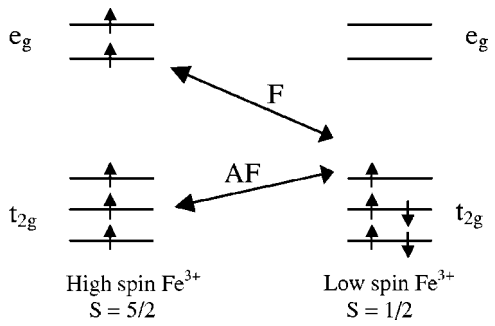


FIG. 8. Distribution of electrons in $t_{2g}$ and $e_g$ orbitals for high spin and low spin $Fe^{3+}$ ions. F indicates ferromagnetic coupling and AF indicates antiferromagnetic coupling among magnetic orbitals.

tiferromagnetic coupling among the magnetic orbitals of the $Fe^{3+}$ ions is shown in Fig. 8. It is, therefore, evident that for the present system ferromagnetic coupling between orbitals of different symmetries is dominant over antiferromagnetic coupling between orbitals of same symmetries and the resultant ordering among the magnetic orbitals is ferromagnetic.

## IV. SUMMARY AND CONCLUSIONS

We have presented the structural and magnetic properties of ferriferricyanide, $Fe[Fe(CN)_6]\cdot 4H_2O$. It is a member of hexacyanometallate based molecular magnetic materials. It crystallizes in the fcc structure with space group $Fm3m$. $Fe^{3+}$ ion octahedrally coordinated by nitrogen atoms is in high spin ($S=5/2$) state and $Fe^{3+}$ ion octahedrally coordinated by carbon atoms is in low spin ($S=1/2$) state. The compound undergoes a paramagnetic to ferromagnetic phase transition at 17.4 K. The observed value of $\mu_{\text{eff}}$, 6.31 $\mu_B$ per formula unit, agrees well with the theoretically expected spin only value of 6.16 $\mu_B$. Saturation magnetization (5.8 $\mu_B$ per formula unit) is in disagreement with the literature reported value of 3.8 $\mu_B$ per formula unit. However, our observed value of saturation magnetization is in agreement with the expected 6 $\mu_B$ per formula unit from collinear ferromagnetic ordering of high spin and low spin $Fe^{3+}$ ions. Coercive field of the compound is an order of magnitude higher than that of many other compounds of the hexacyanometallates family. Thermomagnetic irreversibility between ZFC and FC magnetization curves is observed up to $\sim$5 kOe field. This irreversibility might have its origin in magnetic domain kinetics under different cooling conditions and also due to the presence of available vacant sites in the lattice for the water molecules. The observed ferromagnetism of this compound has been understood qualitatively in terms of molecular field theory. The compound has both ferromagnetic (between orthogonal magnetic orbitals) as well as antiferromagnetic (between the orbitals having the same symmetry) interactions but the ferromagnetic interactions are dominant over antiferromagnetic interactions and the resultant ordering is ferromagnetic.

## ACKNOWLEDGMENTS

The authors are grateful to Dr. M. Ramanadham, Dr. J. V. Yakhmi, and Dr. V. C. Sahni for their encouragement and support in this work.

*Author to whom correspondence shoud be addressed. Fax: +91 22 25505151. Email address: smyusuf@apsara.barc.ernet.in

[1] O. Kahn, *Molecular Magnetism* (VCH, New York, 1993).
[2] J. V. Yakhmi, Physica B **321**, 204 (2002).
[3] S. Ferlay, T. Mallah, R. Ouahes, P. Veillet, and M. Verdaguer, Nature (London) **378**, 701 (1995).
[4] O. Sato, T. Iyoda, A. Fujishima, and K. Hashimoto, Science **271**, 49 (1996).
[5] T. Mallah, S. Thiebaut, M. Verdaguer, and P. Veillet, Science **262**, 1554 (1993).
[6] R. E. William and G. S. Girolami, Science **268**, 397 (1995).
[7] V. Gadet, T. Mallah, I. Castro, and M. Verdaguer, J. Am. Ceram. Soc. **114**, 9213 (1992).
[8] W. R. Entley and G. S. Girolami, Inorg. Chem. **33**, 5165 (1994).
[9] W. D. Griebler and D. Babel, Z. Naturforsch. B **87**, 832 (1982).
[10] M. Verdaguer, A. Bleuzen, V. Marvaud, J. Vaissermann, M. Seuleiman, C. Desplanches, A. Scuiller, C. Train, R. Garde, G. Gelly, C. Lomenech, I. Rosenman, P. Veillet, C. Cartier, and F. Villain, Coord. Chem. Rev. **190–192**, 1023 (1999).
[11] F. Herren, P. Fischer, A. Lüdi, and W. Hälg, Inorg. Chem. **19**, 956 (1980).
[12] H. J. Buser, D. Schwarzenbach, W. Petter, and A. Lüdi, Inorg. Chem. **16**, 2704 (1977).
[13] A. Ito, M. Suenaga, and K. Ono, J. Chem. Phys. **48**, 3597 (1968).
[14] R. M. Bozorth, H. J. Williams, and D. E. Walsh, Phys. Rev. **103**, 572 (1956).
[15] J. Rodriguez-Carvajal, FULLPROF version 3.0.0, LLB CEA-CNRS, 1995.
[16] C. W. Ng, J. Ding, and L. M. Gan, J. Solid State Chem. **156**, 400 (2001).
[17] C. W. Ng, J. Ding, Y. Shi, and L. M. Gan, J. Phys. Chem. Solids **62**, 767 (2001).
[18] C. W. Ng, J. Ding, P. Y. Chow, L. M. Gan, and C. H. Quek, J. Appl. Phys. **87**, 6049 (2000).
[19] J. Ding, C. W. Ng, and Y. Shi, IEEE Trans. Magn. **37**, 2938 (2001).
[20] S. Juszczyk, A. Ratuszna, K. Kaczmarska, G. Matecki, M. Hanson, and C. Johansson, J. Magn. Magn. Mater. **157/158**, 499 (1996).
[21] S.-I. Ohkoshi and K. Hashimoto, Chem. Phys. Lett. **314**, 210 (1999).
[22] T. Wasiutynski, Z. Szeglowski, A. W. Pacyna, and M. Balanda, Physica B **253**, 305 (1998).
[23] C. Y. Huang, J. Magn. Magn. Mater. **51**, 1 (1985).
[24] S. M. Yusuf, L. Madhav Rao, P. L. Paulose, and V. Nagarajan, J. Magn. Magn. Mater. **166**, 349 (1997).
[25] G. G. Kenning, D. Chu, and R. Orbach, Phys. Rev. Lett. **66**, 2923 (1991).
[26] R. V. Chamberlin, M. Hardiman, L. A. Turkevich, and R. Orbach, Phys. Rev. B **25**, 6720 (1982).

[27] H. A. Katori and A. Ito, J. Phys. Soc. Jpn. **63**, 3122 (1994).
[28] S. M. Yusuf, M. Sahana, K. Dörr, U. K. Roßler, and K.-H. Müller, Phys. Rev. B **66**, 064414 (2002).
[29] R. S. Freitas, L. Ghivelder, F. Damay, F. Dias, and L. F. Cohen, Phys. Rev. B **64**, 144404 (2001).
[30] B. J. Hickey, M. A. Howson, S. O. Musa, G. J. Tomaka, B. D. Rainford, and N. Wiser, J. Magn. Magn. Mater. **147**, 253 (1995).
[31] J. C. Denardin, A. L. Brandl, M. Knobel, P. Panissod, A. B. Pakhomov, H. Liu, and X. X. Zhang, Phys. Rev. B **65**, 064422 (2002).
[32] M. D. Mukadam, S. M. Yusuf, P. Sharma, and S. K. Kulshreshtha, J. Magn. Magn. Mater. **269**, 317 (2004).
[33] S. M. Yusuf and L. Madhav Rao, J. Phys.: Condens. Matter **7**, 5891 (1995).
[34] S. M. Yusuf, V. C. Sahni, and L. Madhav Rao, J. Phys.: Condens. Matter **7**, 873 (1995).
[35] T. V. Chandrasekhar Rao, P. Raj, S. M. Yusuf, L. Madhav Rao, A. Sathyamoorthy, and V. C. Sahni, Philos. Mag. B **74**, 279 (1996).
[36] S. M. Yusuf, L. Madhav Rao, R. Mukhopadhyay, S. Giri, K. Ghoshray, and A. Ghoshray, Solid State Commun. **101**, 145 (1997).